Entanglement and level crossings in frustrated ferromagnetic rings

Masudul Haque,[1] V. Ravi Chandra,[1] and Jayendra N. Bandyopadhyay[1,2]

[1]*Max-Planck Institute for the Physics of Complex Systems, Nöthnitzer Str. 38, 01187 Dresden, Germany*
[2]*Department of Physics, National University of Singapore, Singapore 117542, Singapore*

We study the entanglement content of a class of mesoscopic tunable magnetic systems. The systems are closed finite spin-1/2 chains with ferromagnetic nearest-neighbor interactions frustrated by antiferromagnetic next-nearest-neighbor interactions. The finite chains display a series of level crossings reflecting the incommensurate physics of the corresponding infinite-size chain. We present dramatic entanglement signatures characterizing these unusual level crossings. We focus on multispin and global measures of entanglement rather than only one-spin or two-spin entanglements. We compare and contrast the information obtained from these measures to that obtained from traditional condensed-matter quantities such as correlation functions.

I. INTRODUCTION

The study of entanglement in the eigenstates of condensed-matter Hamiltonians is a rapidly growing field of interdisciplinary research [1]. While a great many results have been reported, the typical situation is that entanglement studies of condensed-matter systems provide alternative signatures of phenomena already known from more traditional condensed-matter techniques. In this paper, we use quantities from quantum information to characterize a spin system which is poorly understood in the condensed-matter literature, namely, spin rings with ferromagnetic nearest-neighbor interactions frustrated by antiferromagnetic next-nearest-neighbor interactions. We show how the unusual properties of this system are reflected in quantum information quantities.

The systems we present are closed rings of $N \sim O(10)$ spins. The study of finite-size quantum systems has enjoyed a huge resurgence in the past decade because of cold-atom and nanoscience developments, which provide the context for designing and studying finite-size Hamiltonians for their own fundamental properties rather than as mere tools for investigating the thermodynamic limit $N \rightarrow \infty$. We will focus on a sequence of ground-state level crossings in such systems, which reflect lattice-incommensurate correlations. We show that certain measures of entanglement display remarkably strong parameter dependences near these level crossings. Our calculations of the *concurrence* show that the entanglement structure of the states between successive level crossings is ideal for tuning the distance between spins which are mutually entangled. We also present some results on entanglement *dynamics*, again focusing on the effect of the level crossings.

It is natural to think of ground-state level crossings as finite-size analogs of first-order phase transitions in the thermodynamic limit. As a corollary, one expects that ground-state properties change suddenly at the crossing ("transition") point and that away from the exact crossing point the system possesses no knowledge of the proximity of the crossing. In this regard, our quantum information quantities reveal a peculiarity of the crossings in our spin rings, because they seem to evolve in response to the proximity of the level crossings, already at some distance away from the parameter value where the crossing occurs, i.e., the ground state is "aware" of the nearby crossing. This counterintuitive phenomenon is clearly seen in multispin (but bipartite) entanglements as well as fidelities, but not in traditional condensed-matter quantities such as correlation functions. Note that, since the level crossings are not expected in the thermodynamic limit, this issue is meaningful only in our mesoscopic context.

To calculate a bipartite entanglement, one has to first decide on a partition. For a condensed-matter model or even its finite-size versions, there are a large number of ways in which the system can be bipartitioned. A variety of different partitionings, and correspondingly different entanglements, have been used for entanglement studies in condensed-matter models. Many studies have focused on the entanglement between two sites as measured by the concurrence or negativity (e.g., [2–8]), or the entanglement between one spin or site with the rest (e.g., [9–11]). Such measures generically are not expected to provide information different from traditional condensed-matter quantities such as two-point correlation functions, since these quantities can be related easily to correlation functions (e.g., [5–9]). In this sense, many-site measures are more innovative. Examples are block entanglement in one dimension (1D) [12] and in two dimensions (2D) [13], and more recently studied spatially disconnected partitions such as sublattice entanglement [14] and entanglement between labeled itinerant particles [15]. Such entanglement measures are not easily related to usual correlation functions, and therefore hold the possibility of providing genuinely new tools for probing collective phenomena in many-particle systems. For our finite-sized chains, we will present entanglement results for various partitions, both two site and many site.

The dynamics of entanglement quantifiers in many-particle systems has attracted some attention recently [16], but is still a relatively poorly understood topic, reflecting the general difficulty of nonequilibrium physics in quantum condensed matter. Entanglement dynamics has also gained interest from the quantum information perspective, e.g., in the context of adiabatic quantum computing [17] and in the context of quantum state transfer ("quantum communication") through spin chains [18]. Obviously, the number of different
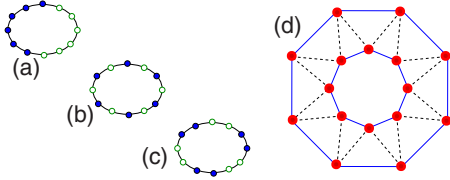
FIG. 1. (Color online) [(a)–(c)] Various partitions of closed chain for calculating bipartite entanglement entropy. Spins belonging to partition A (B) are represented by open (full) circles. (d) Geometry for exploiting the sublattice entanglement $S_{\mathrm{s.l.}}$, e.g., in an experimental realization. In this setup $S_{\mathrm{s.l.}}$ is simply the entanglement between inner and outer rings. Dashed and full lines represent J_1 and J_2 interactions, respectively.

conceivable nonequilibrium situations is large; we are forced to restrict the types of dynamics considered. In this paper we will describe the entanglement dynamics after a sharp change (*quench*) in interaction parameter.

After describing in Sec. II the various entanglement measures and partitions to be used, in Sec. III we introduce the Hamiltonian and its condensed-matter context. Section III also describes the level crossings and compares to other examples of similar crossings known to us. The next sections present entanglement results starting in Sec. IV with the quantities containing the most traditional information, namely, the concurrences which are readily related to correlation functions. Sections V and VI present quantum-information quantities which are more distinct from condensed-matter measures. Section VII describes our results on entanglement dynamics.

II. PARTITIONS AND ENTANGLEMENTS

We will mostly measure entanglement using the *entanglement entropy*. The entanglement entropy between partitions A and B is defined using the reduced density matrix of one part (e.g., $\rho_A = \mathrm{tr}_B\,\rho$ obtained by tracing over B degrees of freedom) to calculate the von Neumann entropy, $S_A = -\mathrm{tr}[\rho_A \ln \rho_A]$. Since the purpose of using entanglement in many-particle systems is to provide viewpoints not present in usual condensed-matter measures, we want to consider more "nonlocal" entanglements. The partitions we choose for this purpose are shown in Fig. 1.

The most obvious choice is for A and B to be spatially connected blocks, in particular for each partition to be a connected half of the ring [Fig. 1(a)]. This partitioning is suggested by many existing results on block entanglement entropies in one dimension [12].

Another choice is to take all the odd sites as partition A and the even sites as partition B—this is then the entanglement between A and B *sublattices*, in usual quantum magnetism language [Fig. 1(b)]. The entanglement between sublattices has been studied for a number of spin chains and lattices and extrema of S_A have been claimed to characterize some quantum phase transitions [14]. Note also that since it is natural to think of the J_1-J_2 chain as a "zigzag ladder" (e.g., [19–21]), the sublattice entanglement is simply the entanglement between the two legs of such a ladder. In the

mesoscopic (finite-size) context that we are interested in, a J_1-J_2 ring is likely to be implemented as shown in Fig. 1(d); the two "legs" are now two J_2 rings (either inner or outer rings, or an upper and a lower layer), connected by zigzag J_1 interactions. From an experimental quantum information processing perspective, the sublattice entanglement is natural as it is simply the entanglement between inner and outer (or upper and lower) rings.

Since the antiferromagnetic interaction in our case is the *next*-nearest-neighbor interaction, we extend the idea of the sublattice partition ($ABAB\ldots$) and also use the $AABBAA\ldots$ partition shown in Fig. 1(c). We call the entanglement entropies corresponding to the above three partitions, respectively, $S_{1/2}$, $S_{\mathrm{s.l.}}$, and $S_{2/4}$.

Another nonlocal quantity motivated by quantum information theory is the fidelity, the overlap between ground-state wave functions at slightly different system parameters [22]. We describe fidelities in our spin rings in Sec. VI.

We also present results for more "local" measures of entanglement, namely, (1) entanglement entropy for two-site partitions and (2) the concurrence C_r measuring the entanglement between sites i and $i+r$ in the environment provided by the rest of the chain [23]. The concurrence is defined as

$$C_r = \max[0,\ (\sqrt{\lambda_1} - \sqrt{\lambda_2} - \sqrt{\lambda_3} - \sqrt{\lambda_4})],$$

where λ_i are the eigenvalues in decreasing order of the matrix $\rho_A(\sigma_y \otimes \sigma_y)\rho_A^*(\sigma_y \otimes \sigma_y)$, and ρ_A is the reduced density matrix of the two-site subsystem. Since we will consider singlet states, two-site reduced density matrices are strongly constrained, and the concurrence is a simple function of the spin-spin correlation functions. Two spins are entangled ($C_r > 0$) if the correlations between them are sufficiently antiferromagnetic, $\langle S_i^z S_{i+r}^z \rangle < -\frac{1}{12}$, and in that case $C_r = -6\langle S_0^z S_r^z \rangle - \frac{1}{2}$ (derived in, e.g., [6,24]; see also Ref. [22] in [21]). The behavior of concurrence in various spin models is briefly reviewed from the literature in Sec. IV in order to provide context for our concurrence results.

We note that the two entanglement quantifiers we use, the entanglement entropy and the concurrence, are both special cases of the *entanglement of formation* [25], the former for pure states and the latter for mixed states [23]. Thus, much of our results can be thought of as a study of the entanglement of formation between various partitions of frustrated ferromagnetic rings.

III. FRUSTRATED FERROMAGNETIC RINGS

We are concerned with closed chains of N localized spin-1/2 objects, i.e., a finite-size spin chain, interacting via the Hamiltonian

$$H = J_1 \sum_i \mathbf{S}_i \cdot \mathbf{S}_{i+1} + J_2 \sum_i \mathbf{S}_i \cdot \mathbf{S}_{i+2}, \tag{1}$$

where $J_1 < 0$, $J_2 > 0$, and i is the site index obeying periodic boundary conditions appropriate to a ring. We express distances in units of lattice spacings and set $\hbar = 1$. We define $\beta = J_2/|J_1|$ and $\bar\beta = \beta^{-1}$. This spin chain is known for any even N to have a singlet ground state for $\bar\beta < 4$ and a $(N+1)$-fold

degenerate ferromagnetic ground-state manifold for $\bar{\beta} > 4$ [26]. At $\bar{\beta} = 4$ a singlet ground state is degenerate with the ferromagnetic manifold; these degenerate states are known exactly [19,26–29].

We will confine ourselves to the singlet region, $\bar{\beta} \in (0,4)$. The numerical results are presented for ring sizes divisible by 4, in order to avoid complications due to the parity of $N/2$. The rings for other even sizes have very similar behavior.

Although far less studied compared to the $J_1 > 0$ case (Majumdar-Ghosh chain), the frustrated ferromagnet Hamiltonian has already been known for some time to possess some peculiar properties [19,26,30–33]. More recently, this model has attracted a fresh surge of theoretical attention [20,34–41], partly due to the appearance of materials whose spin physics is described by this model (see references in [20,34]). Most studies concentrate on finite magnetic fields or finite temperatures and on properties in the thermodynamic limit [20,30–40], or very near the transition point at $\bar{\beta} = 4$ [29,36,41,42].

Proliferation of ground-state level crossings

An unusual feature of the singlet region $\bar{\beta} \in (0,4)$ is the number of ground-state level crossings, which proliferate as we increase the number of spins [26]. For $N = 8, 12, 16, 20, \ldots$ spins, there are, respectively one, two, three, four,… level crossings in this region. A very likely interpretation is that the natural correlations in the chain for $\bar{\beta} \in (0,4)$ are incommensurate with wave vector dependent on β. This incommensurability is resolved in different ways by the different ground states. For larger rings, there are a greater number of possibilities to accommodate the incommensurate correlations into the finite system, and hence the larger number of level crossings. The ground-state lattice momentum alternates between 0 and π in the regions between successive level crossings.

Very similar level crossings appear in other spin models known or thought to have spiral correlations. The examples known to us are (1) the Majumdar-Ghosh chain for $J_2 > 0.5 J_1$ [43]; (2) the "sawtooth" chain of Ref. [44]; (3) the frustrated ferrimagnetic chain of Ref. [45]. This phenomenon of proliferating level crossings in finite-size rings as a result of incommensurate correlations, however, is not widely known or discussed in the condensed-matter literature.

IV. CORRELATION FUNCTIONS AND CONCURRENCES

In this section we present more local quantities, in particular traditional condensed-matter quantities such as spin-spin correlation functions and structure factors, and closely related entanglements such as concurrences.

For singlet states, the correlation function $\langle \mathbf{S_i} \cdot \mathbf{S_j} \rangle$ is three times $\langle S_i^z S_j^z \rangle$; we will discuss the latter as a function of $r = |i - j|$. Between $\bar{\beta} = 0$ and the first crossing, the signs of this quantity have the structure
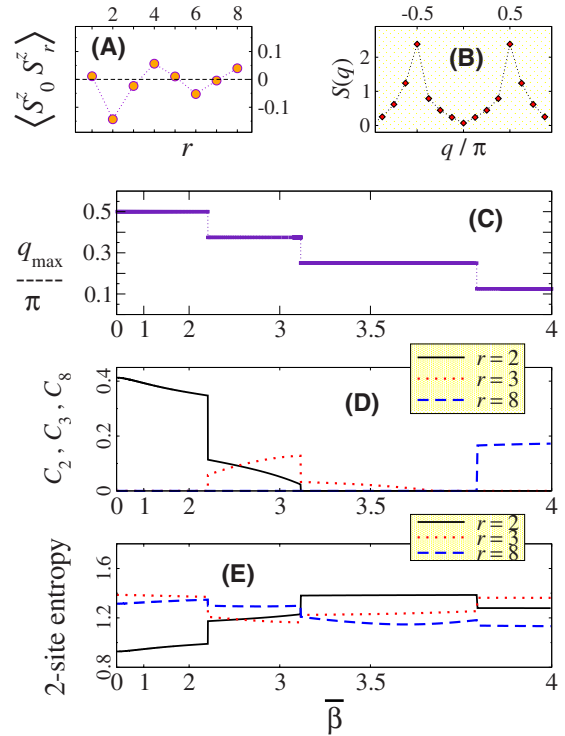
FIG. 2. (Color online) Correlation functions and related quantities for $N = 16$. (a) Correlation function at $\bar{\beta} = 2$. (b) The structure factor, $S(q)$, at $\bar{\beta} = 2$. (c) Position of the maximum of $S(q)$, as a function of $\bar{\beta}$. (d) Concurrences between two spins at distance $r = 2, 3, 8$. (e) Entropy of entanglement between partition consisting of sites (i, $i+r$) and the remaining $N-2$ sites. Shown also for $r = 2, 3, 8$. In (c)–(e), nonlinear horizontal scale highlights the region near $\bar{\beta} = 4$.

$$+ , - , - , + , + , - , - , + , + , \ldots$$

for $r = 1, 2, 3, 4, \ldots$, indicating that the state in this region has a "spin-density-wave"-like $|\uparrow\uparrow\downarrow\downarrow\uparrow\uparrow\ldots\rangle$ structure. An example is shown in Fig. 2(a) for $N = 16$. The oscillating magnitude/sign pattern also suggests "nematic"-like correlations [35,46,47]; detailed distinctions are inappropriate since this is not a macroscopic phase.

The sign pattern of $\langle S_0^z S_r^z \rangle$ changes at each level crossing; for $N = 16$ the patterns in the four regions (separated by level crossings) are

$$+ \quad - \quad - \quad + \quad + \quad - \quad - \quad + ,$$

$$+ \quad - \quad - \quad - \quad + \quad + \quad - \quad - ,$$

$$+ \quad - \quad - \quad - \quad - \quad - \quad + \quad + ,$$

$$+ \quad + \quad + \quad - \quad - \quad - \quad - \quad - .$$

The structure factor $S(q)$, which is the Fourier transform of the real-space correlation function, has peaks at $q_{max} = (2\pi/N)m$, with the integer m decreasing in unit steps at each level crossing, from $m = N/2$ at $\bar{\beta} = 0$ to $m = 1$ near the ferromagnetic transition point [26]. Similar behavior [Fig.

2(c)] is also seen in the other examples known to us where finite-size spin systems have level crossings due to spiral correlations [43,44].

We now consider the concurrences C_r between spins i and $i+r$ on the rings. For most simple spin models, the concurrence does not extend significantly beyond the next-nearest-neighbor site, i.e., $C_{r>2}=0$ for many spin models, such as the *XY* model in transverse field [2], the Heisenberg model ground states on 1D chains and various 2D lattices [6], and even in the Majumdar-Ghosh ($J_1>0$, $J_2>0$) chain [48,49]. In the *XYZ* model in a magnetic field, the concurrence extends to several lattice sites, but still has finite range [50]. Long-range concurrences are rare; the known examples correspond to specific phase transitions [51] or to carefully constructed models and geometries [52,53].

In this context, it is noteworthy that our highly frustrated spin rings display nonzero concurrences at all length scales depending on the interaction parameter $\bar{\beta}$ [Fig. 2(d)]. For any particular value of $\bar{\beta}$, only a couple of concurrences are non-zero, but not necessarily the ones with small r. The r values at which C_r are nonzero, increases as $\bar{\beta}$ changes from 0 to 4, from $r=2$ to $r=N/2$. In the region near the ferromagnetic transition $\bar{\beta}=4$, there is nonzero concurrence between spins at opposite ends of the ring ($C_{r=N/2}>0$), reflecting the unusual long-range quantum correlations of the so-called uniformly distributed resonating valence bond state [19,26] near $\bar{\beta}=4$. The behavior we have found indicates that the interaction here acts as a knob to tune the distance between spins with nonzero entanglement. This tunable distance is quite different from the "entanglement range" of Ref. [51]; our concurrences are not decaying with distance but are nonzero only at a certain distance.

Figure 2(e) shows the entanglement between a two-spin partition (consisting of site i and site $i+r$) and the rest of the ring. Loosely speaking, this entanglement entropy is large (small) when the concurrence *between* the two spins is small (large). This reflects the intuitive idea that objects highly entangled with each other are generally weakly entangled with their environment.

V. ENTANGLEMENTS AND THEIR DERIVATIVES

Figure 3 displays entanglements $S_{1/2}$, $S_{s.l.}$, and $S_{2/4}$ for the partitions explained in Fig. 1, and also the derivatives with respect to $\bar{\beta}$ for the first two cases. The block entanglement entropy $S_{1/2}$ is large compared to, say, the singlet ground state of the nearest-neighbor Heisenberg ground state, in which case $S_{1/2} \sim 1.28(1.354)$ for $N=16(20)$. This is not surprising, as the longer-range interaction causes larger entanglement. The Majumdar-Ghosh chain (positive J_1 and J_2) similarly has relatively large block entanglement [21].

The sublattice entanglement $S_{s.l.}$ starts from zero at $\bar{\beta}=0$, because the two sublattices are decoupled in the $J_2 \to \infty$ limit. After the first level crossing, $S_{s.l.}$ also reaches larger values. Note that $S_{s.l.}$ is quite large in the Heisenberg and Majumdar-Ghosh chains; in comparison the ground-state singlets of our system have somewhat lower sublattice entanglement.
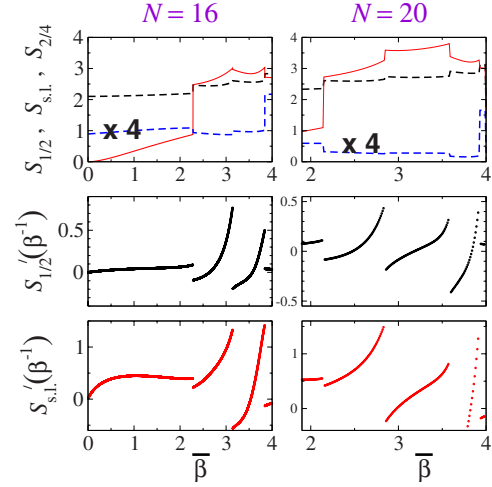
FIG. 3. (Color online) 16-spin and 20-spin rings. Top: half-block and sublattice entanglements, $S_{1/2}$ (upper dashed), $S_{s.l.}$ (solid), $S_{2/4}$ (lower dashed, magnified), against $\bar{\beta}$ in the singlet region. For the $N=20$ curves, smaller values of $\bar{\beta}$ are omitted to focus on the level crossings. Middle and bottom: derivatives of $S_{1/2}(\bar{\beta})$ and $S_{s.l.}(\bar{\beta})$, respectively.

The derivatives of $S_{1/2}(\bar{\beta})$ and $S_{s.l.}(\bar{\beta})$ (Fig. 3 lower panels) are similar and have some striking features. First, at each level crossing except the leftmost, the derivatives have shapes reminiscent of a resonance, although there is no real divergence. In other words, the entanglement curves $S(\bar{\beta})$ become steep but not completely vertical near each crossing. Second, the $S'(\bar{\beta})$ curves appear to respond (curve upward or downward) already some distance away from the level crossing. While phase transition language is not completely appropriate for our mesoscopic arrangements, the crossings in this sense are loosely speaking "second-order" like rather than "first-order" like. Finally, the $S'(\bar{\beta})$ curves at the leftmost crossing lacks the resonancelike feature, indicating that the first level crossing is different in nature.

The $S_{2/4}$ entanglement entropy is peculiarly small (shown fourfold magnified in Fig. 3), although the relevant reduced density matrix has the same dimensions as the other two partitions. This peculiarity remains unexplained at present.

VI. FIDELITIES

The ground-state fidelity is defined as the overlap between ground-state wave functions at nearby parameter values:

$$F_\epsilon(\bar{\beta}) = \left\langle \psi\left(\bar{\beta} - \tfrac{1}{2}\epsilon\right) \middle| \psi\left(\bar{\beta} + \tfrac{1}{2}\epsilon\right) \right\rangle.$$

Recent studies indicate that the fidelity provides useful signatures of quantum phase transitions [22]. Since we concentrate on mesoscopic spin structures, our purpose is not to study phase transitions but to present fidelity signatures of the level crossings.

Figure 4 presents fidelity data for $\epsilon=10^{-3}$. The derivatives $F'(\bar{\beta})$ again show striking resonancelike features. The special nature of the leftmost crossing is manifested even more
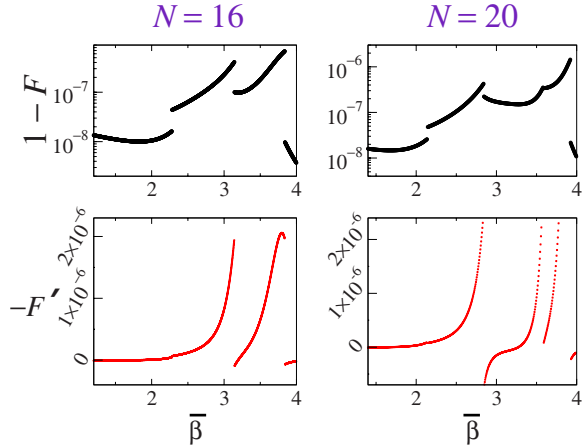
FIG. 4. (Color online) Fidelity $F_\epsilon(\bar\beta)$ with $\epsilon = 10^{-3}$, and its derivative. Since F is generally very close to unity, it is more convenient to plot $1 - F$ on a logarithmic scale. Note that the discontinuity at the leftmost level crossing is pronounced in the fidelity but almost invisible in its derivative.

FIG. 5. (Color online) Left panel shows sublattice entanglement entropy for $N = 12$. Center (rightmost) panel shows evolution of $S_{\text{s.l.}}$ after a quench, without (with) dissipation. Time is expressed in units $|J_1|^{-1}$. Initial values are $\bar\beta_i = 0.5$ (solid), $\bar\beta_i = 3.5$ (dotted), and $\bar\beta_i = 3.85$ (dashed). Final value is $\bar\beta_f = 2.0$ in each case. Damping constant in rightmost panel is shown for $\gamma = 0.5$ for all three $\bar\beta_i$. For $\bar\beta_i = 0.5$, the thick solid line has smaller damping, $\gamma = 0.1$. In the presence of dissipation, $S_{\text{s.l.}}$ relaxes to the ground-state value when the initial state has same lattice momentum ($k = \pi$) but not when the initial state has different lattice momentum ($k = 0$).

dramatically here—the derivatives match almost perfectly across this crossing, even though the fidelities themselves are discontinuous.

VII. TIME EVOLUTION AFTER A QUENCH

We now turn to the *dynamics* of entanglement in the frustrated ferromagnetic chain. While each entanglement quantifier has its own dynamics when the quantum state of the spin ring evolves outside equilibrium, a full study of the dynamics of all such quantities is outside the scope of the present investigation, especially since such comprehensive entanglement dynamics studies are yet to be completed for simpler spin systems. We therefore restrict the presentation to the dynamics of the sublattice entanglement entropy ($S_{\text{s.l.}}$).

The fact that our system has true level crossings places them in the complete opposite limit to what is necessary for adiabatic quantum computing [17]. It is therefore perhaps natural to study the opposite limit of adiabatic parameter changes, namely, parameter *quenches* where $\bar\beta$ changes as a step function. In an isolated finite spin ring, a quench of this type leads to oscillatory behaviors of most quantities, including entanglement entropies for various partitions; there is no relaxation mechanism for the system to reach its ground state. This is shown in Fig. 5 (center panel). Studying the evolution after a parameter quench from β_i to β_f involves following the wave function

$$|\psi(t)\rangle = \exp[-iH(\beta_f)t]|\psi(0)\rangle$$

explicitly in time, where the initial state $|\psi(0)\rangle$ is the ground state of $H(\beta_i)$. We performed this calculation by expanding the operator $e^{-iH(\beta_f)t}$ to sufficiently high order for each time step.

We also explore relaxation issues, specifically the effect of the 0-π-0-π crossings, by adding an artificial dissipation to the temporal evolution (Fig. 5 rightmost panel). Instead of evolving in time t, we evolve in $t(1 - i\gamma)$. This form of damp-

ing ("cooling") preserves the lattice momentum but not the energy. We display entanglement evolutions for the large-damping case of $\gamma = 0.5$, and also a single example with smaller damping, $\gamma = 0.1$. With damping, the sublattice entanglement $S_{\text{s.l.}}(t)$ relaxes to the ground state $S_{\text{s.l.}}$ corresponding to the final $\bar\beta$ only if the starting state has the same lattice momentum k. For $N = 12$, two level crossings divides the parameter space into regions I and III with the same $k = \pi$ and an intermediate region II with $k = 0$. The entanglement entropy after a quench to $\bar\beta = 2$ (region I) relaxes to the "correct" value if the starting ground state is in region I or III, but not if it is in region II. The structure of level crossings and alternating ground-state momenta thus allow selective targeting of quantum ground states, and therefore could serve as the basis of selective variations of the basic idea behind adiabatic quantum computing.

VIII. CONCLUSIONS

We have identified a mesoscopic system with unusual entanglement properties. Our system is the finite-size analog of the intriguing ferromagnetic-antiferromagnetic chain. The surprising long-distance concurrence we have found, with tunable distance, makes this system ideal for various quantum information processing tasks. For example, *entanglement transport* is here simply a matter of tuning the interaction parameter while remaining in the ground state. Our calculations of multiqubit entanglement entropies and the fidelities have revealed unexpected aspects of the level crossings present in these systems. We have also presented entanglement dynamics results, again indicating possible quantum information processing applications.

Our work opens up a number of questions. First, our focus on the 0-π-0-π-level crossings raises the following ques-

tion: which of the entanglement behaviors reported here also carry over to the other systems where such level crossings have been observed? To the best of our knowledge, no unified study of such crossings exists. Our entanglement results call for a general investigation of finite-size level crossing sequences occurring as a result of incommensurate correlations.

Second, our study of entanglement dynamics treats only a minute fraction of the possible kinds of dynamics and only a single entanglement measure out of many. Since entanglement estimators are sensitive to a variety of wave function characteristics not necessarily present in traditional condensed-matter measures such as correlation functions, the dynamics of these new measures present rich opportunities for characterizing nonequilibrium phenomena. Again, comprehensive investigations are called for, but the study of the evolution of various entanglements would be appropriately first done in simpler (perhaps exactly solvable) many-body systems.

[1] L. Amico, R. Fazio, A. Osterloh, and V. Vedral, Rev. Mod. Phys. **80**, 517 (2008).

[2] A. Osterloh, L. Amico, G. Falci, and R. Fazio, Nature (London) **416**, 608 (2002).

[3] T. J. Osborne and M. A. Nielsen, Phys. Rev. A **66**, 032110 (2002).

[4] I. Bose and E. Chattopadhyay, Phys. Rev. A **66**, 062320 (2002).

[5] O. F. Syljuasen, Phys. Rev. A **68**, 060301(R) (2003).

[6] V. Subrahmanyam, Phys. Rev. A **69**, 022311 (2004).

[7] S. Y. Cho and R. H. McKenzie, Phys. Rev. A **73**, 012109 (2006).

[8] X. Wang and P. Zanardi, Phys. Lett. A **301**, 1 (2002).

[9] A. Kopp and K. Le Hur, Phys. Rev. Lett. **98**, 220401 (2007).

[10] A. Tribedi and I. Bose, Phys. Rev. A **75**, 042304 (2007).

[11] S. Alipour, V. Karimipour, and L. Memarzadeh, Phys. Rev. A **75**, 052322 (2007).

[12] G. Vidal, J. I. Latorre, E. Rico, and A. Kitaev, Phys. Rev. Lett. **90**, 227902 (2003); J. I. Latorre, E. Rico, and G. Vidal, Quantum Inf. Comput. **4**, 48 (2004); V. E. Korepin, Phys. Rev. Lett. **92**, 096402 (2004); P. Calabrese and J. Cardy, J. Stat. Mech.: Theory Exp. (2004), P06002.

[13] D. Gioev and I. Klich, Phys. Rev. Lett. **96**, 100503 (2006); M. M. Wolf, *ibid.* **96**, 010404 (2006); T. Barthel, M.-C. Chung, and U. Schollwöck, Phys. Rev. A **74**, 022329 (2006); A. Kitaev and J. Preskill, Phys. Rev. Lett. **96**, 110404 (2006); M. Levin and X. G. Wen, *ibid.* **96**, 110405 (2006); E. Fradkin and J. E. Moore, *ibid.* **97**, 050404 (2006).

[14] Y. Chen, Z. D. Wang, and F. C. Zhang, Phys. Rev. B **73**, 224414 (2006); Y. Chen, P. Zanardi, Z. D. Wang, and F. C. Zhang, New J. Phys. **8**, 97 (2006).

[15] H. M. Wiseman and J. A. Vaccaro, Phys. Rev. Lett. **91**, 097902 (2003); M. R. Dowling, A. C. Doherty, and H. M. Wiseman, Phys. Rev. A **73**, 052323 (2006); Y. Shi, J. Phys. A **37**, 6807 (2004); M. Haque, O. Zozulya, and K. Schoutens, Phys. Rev. Lett. **98**, 060401 (2007); H. Katsura and Y. Hatsuda, J. Phys. A **40**, 13931 (2007); R. Santachiara, F. Stauffer, and D. Cabra, J. Stat. Mech.: Theory Exp. (2007), L05003.; O. S. Zozulya, M. Haque, and K. Schoutens, Phys. Rev. A **78**, 042326 (2008).

[16] A. M. Läuchli and C. Kollath, J. Stat. Mech.: Theory Exp. 2008, P05018.; P. Calabrese and J. Cardy, *ibid.* (2007), P06008.; G. De Chiara, S. Montangero, P. Calabrese, and R. Fazio, *ibid.* (2006), P03001.; P. Barmettler, A. Rey, E. Demler, M. Lukin, I. Bloch, and V. GritsevPhys. Rev. A **78**, 012330 (2008); L. Amico, A. Osterloh, F. Plastina, R. Fazio, and G. M. Palma, *ibid.* **69**, 022304 (2004).

[17] E. Farhi, J. Goldstone, S. Gutmann, J. Lapan, A. Lundgren, and D. Preda, Science **292**, 472 (2001); E. Farhi, J. Goldstone, S. Gulmann, and M. Sipser, e-print arXiv:quant-ph/0001106.

[18] S. Bose, Contemp. Phys. **48**, 13 (2007).

[19] T. Hamada *et al.*, J. Phys. Soc. Jpn. **57**, 1891 (1988).

[20] H. T. Lu, Y. J. Wang, S. Qin, and T. Xiang, Phys. Rev. B **74**, 134425 (2006).

[21] R. W. Chhajlany, P. Tomczak, A. Wójcik, and J. Richter, Phys. Rev. A **75**, 032340 (2007).

[22] P. Zanardi and N. Paunkovic, Phys. Rev. E **74**, 031123 (2006); P. Buonsante and A. Vezzani, Phys. Rev. Lett. **98**, 110601 (2007); M. Cozzini, P. Giorda, and P. Zanardi, Phys. Rev. B **75**, 014439 (2007); M. Cozzini, R. Ionicioiu, and P. Zanardi, *ibid.* **76**, 104420 (2007); M.-F. Yang, *ibid.* **76**, 180403(R) (2007).

[23] W. K. Wootters, Phys. Rev. Lett. **80**, 2245 (1998).

[24] S.-J. Gu, H.-Q. Lin, and Y.-Q. Li, Phys. Rev. A **68**, 042330 (2003).

[25] C. H. Bennett, D. P. DiVincenzo, J. A. Smolin, and W. K. Wootters, Phys. Rev. A **54**, 3824 (1996).

[26] T. Tonegawa and I. Harada, J. Phys. Soc. Jpn. **58**, 2902 (1989).

[27] D. V. Dmitriev, V. Ya. Krivnov, and A. A. Ovchinnikov, Phys. Rev. B **56**, 5985 (1997).

[28] D. V. Dmitriev, V. Ya. Krivnov, and A. A. Ovchinnikov, Phys. Rev. B **61**, 14592 (2000).

[29] H. Suzuki and K. Takano, J. Phys. Soc. Jpn. **77**, 113701 (2008).

[30] A. V. Chubukov, Phys. Rev. B **44**, 4693 (1991).

[31] D. C. Cabra, A. Honecker, and P. Pujol, Eur. Phys. J. B **13**, 55 (2000).

[32] A. A. Nersesyan, A. O. Gogolin, and F. H. L. Essler, Phys. Rev. Lett. **81**, 910 (1998).

[33] C. Itoi and S. Qin, Phys. Rev. B **63**, 224423 (2001).

[34] F. Heidrich-Meisner, A. Honecker, and T. Vekua, Phys. Rev. B **74**, 020403(R) (2006).

[35] T. Vekua, A. Honecker, H.-J. Mikeska, and F. Heidrich-Meisner, Phys. Rev. B **76**, 174420 (2007).

[36] D. V. Dmitriev and V. Ya. Krivnov, Phys. Rev. B **73**, 024402 (2006).

[37] L. Kecke, T. Momoi, and A. Furusaki, Phys. Rev. B **76**, 060407(R) (2007).

[38] M. Hartel, J. Richter, D. Ihle, and S. L. Drechsler, Phys. Rev. B **78**, 174412 (2008).

[39] T. Hikihara, L. Kecke, T. Momoi, and A. Furusaki, Phys. Rev. B **78**, 144404 (2008).

[40] J. Sudan, A. Luscher, and A. Laeuchli, e-print arXiv:0807.1923. A. M. Laeuchi, J. Sudan, and A. Luscher, J. Phys.: Conf. Ser. **145**, 012057 (2009).

[41] S. Mahdavifar, J. Phys.: Condens. Matter **20**, 335230 (2008).

[42] V. Y. Krivnov and A. A. Ovchinnikov, Phys. Rev. B **53**, 6435 (1996).

[43] T. Tonegawa and I. Harada, J. Phys. Soc. Jpn. **56**, 2153 (1987).

[44] V. R. Chandra, D. Sen, N. B. Ivanov, and J. Richter, Phys. Rev. B **69**, 214406 (2004).

[45] N. B. Ivanov, J. Richter, and U. Schollwöck, Phys. Rev. B **58**, 14456 (1998).

[46] N. Shannon, T. Momoi, and P. Sindzingre, Phys. Rev. Lett. **96**, 027213 (2006).

[47] T. Momoi and N. Shannon, Prog. Theor. Phys. **159**, 72 (2005).

[48] S.-J. Gu, H. Li, Y.-Q. Li, and H.-Q. Lin, Phys. Rev. A **70**, 052302 (2004).

[49] X.-F. Qian, T. Shi, Y. Li, Z. Song, and C.-P. Sun, Phys. Rev. A **72**, 012333 (2005).

[50] T. Roscilde, P. Verrucchi, A. Fubini, S. Haas, and V. Tognetti, Phys. Rev. Lett. **93**, 167203 (2004).

[51] L. Amico, F. Baroni, A. Fubini, D. Patane, V. Tognetti, and P. Verrucchi, Phys. Rev. A **74**, 022322 (2006).

[52] L. Campos Venuti, C. Degli Esposti Boschi, and M. Roncaglia, Phys. Rev. Lett. **96**, 247206 (2006).

[53] L. Campos Venuti, S. M. Giampaolo, F. Illuminati, and P. Zanardi, Phys. Rev. A **76**, 052328 (2007).